

## Research Article

# CAD Interior Design Color Transfer Simulation Based on the Topological Information Area Matching Model

**Mingyan Wang** 

*Yancheng Polytechnic College, Yancheng 224005, China*

Correspondence should be addressed to Mingyan Wang; wangmingyan2021@hotmail.com

Received 18 November 2021; Revised 17 December 2021; Accepted 27 December 2021; Published 17 March 2022

Academic Editor: Qiangyi Li

Copyright © 2022 Mingyan Wang. This is an open access article distributed under the Creative Commons Attribution License, which permits unrestricted use, distribution, and reproduction in any medium, provided the original work is properly cited.

With the continuous development of social economy, interior design has gradually become an important content pursued by people, especially the rise of European and American style, industrial style, and other design styles, which have a greater impact on the style of interior design. In view of these needs and limitations, a topological information area matching model is introduced by trial in this study. The relationship of area matching is defined by trial through combining the business analysis flow of interior design, accurately controlling the importance of color transfer, and effectively performing the effective transfer of coloring according to the matching area, to improve the integrity of the color transfer, reduce the influence of the variegation in the color transfer on the result according to the mutually harmonious color method, and significantly improve the mutual harmony of colors. The simulation experiment results show that the topological information area matching model is effective, can ensure the true color of the image color, can be effectively adjusted according to the local matching relationship and color, and can support the simulation of CAD interior design color transfer.

## 1. Introduction

With the continuous development of social economy, people have higher and higher requirements for interior design and decoration. In recent years, design styles such as industrial style and European and American style have brought many revolutionary changes to interior design [1, 2]. In the field of interior design, how to ensure the effective transfer of colors is extremely important. The so-called color transfer is to use statistics or color models to transfer the color of the target image to the original image. The image after the color transfer and the target color image are subjected to effective or similar color statistical information so that statistics is performed for the color image after transferring, that is, the color statistics of the target image, which can realize the transfer of the target color, and it is meaningful for the color design of the product. For color transfer, we can mainly classify global color transfer and locally segmented color transfer [3].

In the field of global color transfer, some scholars within the industry adjust the parameters and calculate the image

matrix by setting the scaling factor, average value, etc., in order to improve the effect of color transfer. For example, to achieve the contrast between image pixel spatial information and color information through gradient maintenance, it is necessary to fully consider the size of the color image. If the number of images is too large, more time will be consumed on the relative overall image. On this basis, some scholars use manual interactive evaluation, linear template mapping evaluation, and image probability model evaluation, to achieve effective color transfer between scenes and carry out image similarity analysis, but these methods have higher requirements for the original quality of the image. Therefore, in the specific interior design process, CAD interior design has many advantages, which can realize the design reproduction of planning layout and simulation, but there are still certain limitations and deficiencies [4, 5].

In the color transfer of local segmentation, in order to effectively realize that the uncontrollable color transfer of the global algorithm, some scholars use image segmentation methods to match color transfer, that is, segmentation is achieved through mathematical modeling, and gray

information indicators are used to perform regional matching and finally complete the color transfer [6]. In addition, some scholars use the delineation method to operate the image area and realize the effectiveness of color transfer through manual interaction; for example, the fuzzy clustering algorithm is used to segment the image color, and the weighted pixel color analysis is realized according to the degree of membership to realize the consumed effective color transfer of natural scene pictures [7]. On this basis, some scholars have stylized the image color based on the specific color themes formed by the specific style vocabulary to transform the image color in the styles. However, the transferred colors are fixed because of this method, and the effect of transfer of those ones with relatively rich color or too single ones is poor, so it is necessary to distinguish the overall perception of the image from the overall perspective.

The main essence of the color transfer of local segmentation is to use the specific mean value of the region as an index of image matching, so as to effectively match the neighboring regions with similar brightness values. When the number of specific segmented regions is equal, the reasonable legality of the corresponding matching regions is realized. In response to these shortcomings and needs, based on the topological comprehensive information matching model, by overcoming the color easily lost in global algorithm, while avoiding the disadvantages of poor effects caused by the partial segmentation of color transfer, the importance of color transfer is controlled accurately, and effective color transfer is performed according to the matching area, and corresponding adjustments are made according to the input color area to improve the integrity of the color transfer; the influence of the variegation in the color transfer is reduced on the result based on the mutually harmonious color method, aiming to effectively improve effectiveness and efficiency of interior design.

## 2. Flow of the Algorithm in This Paper

The algorithm steps in this paper are as follows:

Input: original image and target color image.

Output: the image after color transfer.

Step 1: first, perform effective area division for the input image, and on this basis, clarify the topological relationship between each area and use the corresponding matching strategy to analyze and determine the corresponding relationship between the area matching. If the result of the matching is not satisfied, the initial area of the matching is realized according to the specific interaction of the user, so as to realize the subsequent matching process according to the specific topological adjacency and improve the effectiveness and accuracy of the color transfer.

Step 2: on the basis of step 1, the color adjustment of the unmatched area is realized to improve the integrity of the color transfer according to the analysis of the color transfer of the matched corresponding area.

Step 3: on the basis of step 2, a harmonious color model is used to specifically solve the problem of variegation in color transfer, as well as the problem of inharmonious colors in the small color in the image due to lack of adjusting area, and focus on solving the degree of harmony in color transfer.

On the basis of this step, the problem of insufficient color in the global algorithm is changed in this study, and in the meantime, the problem of the different numbers of image segmentation in the local algorithm is avoided, and a more complete area matching method is proposed for complex color scenes. Based on color adjustment and the harmony of colors, the final result of color transfer is enhanced.

## 3. Regional Matching Based on Topological Comprehensive Information

The first is to distinguish the color of the indoor scene area and analyze the characteristics of rich colors. To some extent, the global color transfer method can only obtain a relatively single-color transfer result. In this study, the corresponding algorithm is used to effectively segment the local area, realize the topological segmentation of the area, and guide the correlation matching of the area to obtain the specific correspondence. In the interior scene design, the area between various colors is more distinct than the natural scene, and the division of each area is also clearer [8]. Therefore, the corresponding algorithm is used to divide the region, establish a mixed Gaussian model, and realize achieve better segmentation by making use of interaction.

Assuming that  $V_i$  represents the topological matching vector of the  $i$ th region and its expression is  $V_i = (N_i, R_i, \omega_L L_i, \omega_S S_i)$ , then the specific calculation can be carried out in detail by the following formula:

$$\left\{ \begin{array}{l} N_i = \frac{n_i}{n_t} \\ R_i = \frac{a_i}{(I_w \times I_h)} \\ L_i = \frac{\bar{L}_i}{(L_D/2)} \\ S_i = \frac{\sum_{j \in \psi} R_j D(c_i, c_j)}{256} \end{array} \right. \quad (1)$$

In order to obtain the matching relationship  $F$ , the specific calculation of the energy function is shown in the following formula:

$$F = \min_F \left( \|V_i^s - V_j^t\|^2 \right). \quad (2)$$

When the target color image is divided and combined to exceed the number of original image areas, it can be discarded according to the remaining area of the target color image. When the number of divided areas of the target color

image is less than the number of original image areas, it can be effectively adjusted according to the specific methods.

Simply matching regions through topological relationships often results in too large differences in the scene structure and unreasonable results. Therefore, for this specific situation, the following improvements can be made:

Step 1: through the human-computer interaction, the matching mapping relationship of the specific part of the area can be clarified, that is, the selection of the area for interior design, typically such as floor and ceiling.

Step 2: according to the determined matching relationship, restrict the matching operation of the remaining area in its adjacent area.

Step 3: if there is a remaining area, it is specifically matched and solved according to formula (2).

According to the abovementioned regional matching algorithm, specific matching is implemented and analyzed from the analyzed topological adjacency relationship, and the subsequent matching result analysis is set, so there is no specific and reasonable matching result.

In the specific interactive area process, usually only fixed indoor scenes are selected for distinction, such as the floor. For other areas, such as curtains and cabinets, specific energy functions need to be matched to obtain the overall effect. The proportion of the number of adjacent regions in each region of the target image is shown in Figure 1, and the proportion of the number of adjacent regions in each region of the original image in Figure 1 is shown in Figure 2.

#### 4. Principle of Similarity Evaluation Algorithm Based on Optimal Matching of 3D CAD Models

4.1. *Model Representation.* For the representation of the CAD model system, the 3D CAD model can usually be identified by the geometric method of the structural entity and the B-Rep model. Among them, the structural entity geometry method uses the primitive voxel Boolean operation to express the whole, but because the algorithm is relatively easy, these commercial 3D CAD modeling systems are all applied to analysis. However, for the number of the same model of structural entities, different structures may lead to different conclusions. For the B-Rep model, the finite space enclosed by a closed boundary has the advantage of containing more information about faces, edges, points, and relationships. To evaluate specific information, the B-Rep model is chosen in this study.

4.2. *Analysis and Expression of Model Similarity Factors.* For the CAD model, the similarity is relatively vague, and its essence is to include the similarity of human visual perception and the similarity of specific engineering attributes. The similarity of two CAD models needs to be measured from multiple angles, which is the synthesis

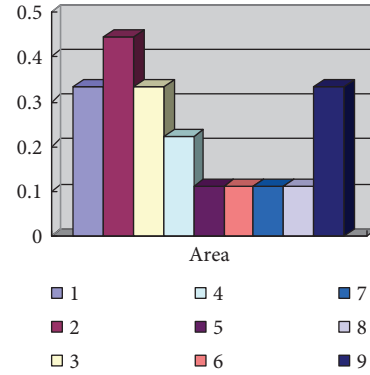


FIGURE 1: Proportion of the number of adjacent areas in each area of the target image.

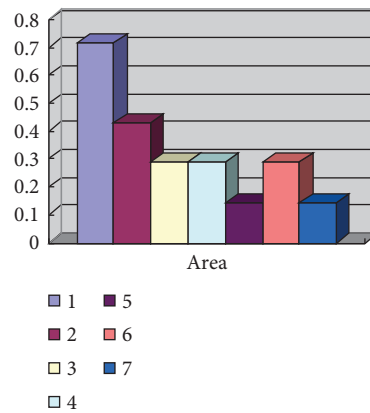


FIGURE 2: Proportion of the number of adjacent regions in each region of the original image in Figure 1.

and expression of multiple information of the model. It can be divided into geometric attributes and topological attributes. In order to evaluate the specific similarity between models in an appropriate and objective way, these two attributes should be considered comprehensively. The B-Rep model can be regarded as an assembly formed by connecting surfaces in different directions through certain rules. Therefore, if the surface shapes of the two models are similar and the connection methods are similar or convergent, the models can be considered similar [9, 10].

4.2.1. *Splitting the Surface.* The B-Rep model encloses and forms surfaces according to a certain relationship and can effectively split the model to be compared into faces and effectively classify them according to specific rules.

4.2.2. *Matching and Abstraction of Surface.* Similar surfaces in the two models are paired. The matrix shown in formula (1) can be identified by the similar matrix in Figure 3. The number of surfaces in the assembly in Figure 3 is not exactly the same. It needs to be completed to make the matrix a square matrix for subsequent processing:

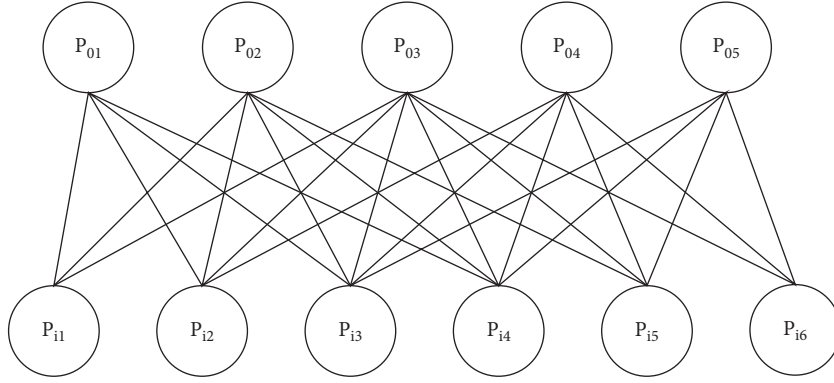


FIGURE 3: The bipartite graph formed by the pairing of plane sets in the two models.

$$M_{0i} = \begin{matrix} & P_{i1} & P_{i2} & P_{i3} & P_{i4} & P_{i5} & P_{i6} \\ \begin{matrix} P_{01} \\ P_{02} \\ P_{03} \\ P_{04} \\ P_{05} \\ 0 \end{matrix} & \begin{bmatrix} \delta_{11} & \delta_{12} & \delta_{13} & \delta_{14} & \delta_{15} & \delta_{16} \\ \delta_{21} & \delta_{22} & \delta_{23} & \delta_{24} & \delta_{25} & \delta_{26} \\ \delta_{31} & \delta_{32} & \delta_{33} & \delta_{34} & \delta_{35} & \delta_{36} \\ \delta_{41} & \delta_{42} & \delta_{43} & \delta_{44} & \delta_{45} & \delta_{46} \\ \delta_{51} & \delta_{52} & \delta_{53} & \delta_{54} & \delta_{55} & \delta_{56} \\ 0 & 0 & 0 & 0 & 0 & 0 \end{bmatrix} \end{matrix} \quad (3)$$

**4.2.3. Optimal Matching and Calculation of Surface Sets.** The similarity of the two models should be determined by the optimal plan for the overall pairing of the same type of surfaces, rather than the optimal specific individual surfaces of the pairing.

**4.2.4. Calculation of Similarity Coefficient of Two Models.** As shown in Figure 3, to compare the similarity of the specific two models, the optimal matching weight of each surface set should be selected for comprehensive evaluation. The specific weight is calculated by the following formula:

$$\Delta x = \sum_{j=1}^n \delta_{n(j)j} \left( \frac{S_{em(j)} + S_{ej}}{2} \right). \quad (4)$$

The relative area of the  $j$ th surface of the same surface in the model Model<sub>i</sub> is calculated as the following formula:

$$S_{ei} = \frac{S_i}{\sum_{j=1}^n S_j}. \quad (5)$$

On the basis of formula (5), calculate the similarity coefficient of each plane type, cylindrical surface type, conical surface type, torus surface type, spherical surface type, and free-form surface type. The specific calculation is as shown in the following formula:

$$\Delta_{0i} = \Delta_{PL} + \Delta_{CY} + \Delta_{CO} + \Delta_{TR} + \Delta_{SP} + \Delta_{FR}. \quad (6)$$

The obtained results are used as the similar parameters of the two models so that the original model and the

comparison model can be used to calculate the similarity coefficients.

**4.3. Analysis and Calculation of Surface Similarity Factors.** Describe the dissimilarity of the two quantities  $a$  and  $b$  ( $a \geq 0$ ,  $b \geq 0$ ); the calculation is as shown in the following formula:

$$d(a, b) = \frac{|a - b|}{\max(a, b)}. \quad (7)$$

When one of  $a$  or  $b$  is 0, the dissimilarity value between  $a$  and  $b$  is 1 regardless of the amount of the other. In this study, formula (8) is used to calculate the similarity quantitatively. The specific calculation is as shown in the following formula:

$$s(a, b) = \begin{cases} 1 - \frac{|a - b|}{\max(a, b)}, & a > b \text{ and } b > 0, \\ 1 - \frac{|a - b|}{\max(a + 1, b + 1)}, & a = 0 \text{ and } b = 0, \\ 0, & a = 0 \text{ and } b = 0 \end{cases} \quad (8)$$

where the specific similarity coefficient that can be calculated for the degree of similarity can be comprehensively considered through the following factors.

**4.3.1. Area Factor.** Since the absolute area of the surface is affected by the size of the model, the relative area is used here, that is, the area of the surface divided by the total surface area of the model.

The similarity  $s_{ij}$  between the area of the  $i$ th surface and the  $j$ th surface is calculated by

$$s_{ij} = 1 - \frac{|s_{ei} - s_{ej}|}{\max(s_{ei}, s_{ej})}. \quad (9)$$

**4.3.2. The Shape Factor of the Surface.** The shape factors of the surface mainly include the number of sides of the surface, the change of the side length of the surface, and the angle between the sides. As shown in Figure 4, the corresponding shape is also different from left to right due to the different

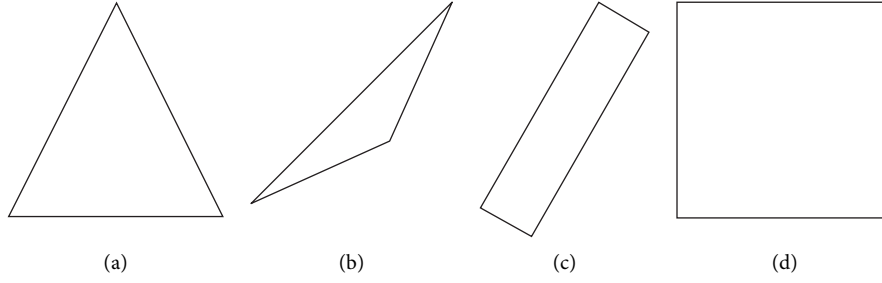


FIGURE 4: The shape factor of the surface.

amounts of side length change [11–13]. The specific calculation can be carried out by the following methods.

Taking Figure 4 as an example, due to the difference in side length changes, Figures 4(a)–4(d) are different. They can be calculated as follows.

(1) *The Influence of the Number of Edges on the Shape.* The number of sides of the two surfaces is represented by  $n_{ei}$  and  $n_{ej}$ , respectively, and the similarity of the number of sides of the two surfaces can be calculated by the following formula:

$$s_{enij} = 1 - \frac{|n_{ei} - n_{ej}|}{\max(n_{ei}, n_{ej})}. \quad (10)$$

(2) *The Influence of the Change of Side Length on the Shape.* Because the side length changes of the two surfaces are different, it is easy to cause the difference in shape. Therefore, the specific quantitative definition of the specific side length similarity is calculated by the following formula:

$$s_{elij} = 1 - \frac{|\delta_i - \delta_j|}{\max(\delta_i, \delta_j)}, \quad (11)$$

where  $\delta_i = \sqrt{1/n \sum_{i=1}^n (x_i - x)^2}$ ,  $x = 1/n \sum_{i=1}^n x_i$ ,  $x_i$  is the length of each side, and  $n$  is the number of sides of the surface.

(3) *Topological Connection of Surfaces.* The topological structure of the CAD indoor model is extremely important in the specific model similarity evaluation process [14, 15]. Therefore, for the B-Rep model, it can be expressed in a specific topological relationship.

In terms of the topological similarity of the two models, a specific model can be used to evaluate and analyze the topological similarity between surfaces. The specific similarity can be specifically calculated by the following formula:

$$s_{tij} = \frac{n_{ecij}}{\max(n_{ei}, n_{ej})}, \quad (12)$$

where  $n_{ecij}$  represents the number of compatible edges in the two surfaces and  $n_{ei}$  and  $n_{ej}$  represent the number of edges of the two compared surfaces, respectively.

The conditions satisfied by the angle  $\theta_1$  and  $\theta_2$  between the two surfaces connected by each of the compatible edges can be calculated by the following formula:

$$|\theta_1 - \theta_2| \leq \varepsilon, \quad (13)$$

where  $\varepsilon$  is a threshold that meets a certain accuracy, as shown in Figure 5.

(4) *Calculation of Similarity Coefficient of Surfaces.* The similarity coefficient  $\delta_{ij}$  between a pair of surfaces that belong to different models but the same type can be calculated according to the following formula:

$$\delta_{ij} = \alpha_s s_{sij} + \alpha_{en} s_{enij} + \alpha_{el} s_{elij} + \alpha_t s_{tij}, \quad (14)$$

where  $\alpha_s$ ,  $\alpha_{en}$ ,  $\alpha_{el}$ , and  $\alpha_t$  are the weights of each item, respectively, and the effect is better when  $\alpha_s = 0.1$ ,  $\alpha_{en} = 0.3$ ,  $\alpha_{el} = 0.1$ , and  $\alpha_t = 0.5$ .

#### 4.4. Color Transfer and Unmatched Area Color Adjustment.

After obtaining the corresponding image matching relationship, according to the number of specific area divisions, it can be divided into two specific situations:

- (1) The number of divided regions of the target color image is greater than or equal to the number of regions in the original color image.

According to the matching relationship, the effective color transfer of pixels is performed in the corresponding color space.

The calculation formula of each channel through color transfer can be calculated by the following formula:

$$\left\{ \begin{array}{l} l'_z = (l_z - \mu_{sl}^i) \frac{\sigma_{tl}^j}{\sigma_{sl}^i} + \mu_{tl}^j \\ \alpha'_z = (\alpha_z - \mu_{sa}^i) \frac{\sigma_{t\alpha}^j}{\sigma_{sa}^i} + \mu_{t\alpha}^j \\ \beta'_z = (\beta_z - \mu_{s\beta}^i) \frac{\sigma_{t\beta}^j}{\sigma_{s\beta}^i} + \mu_{t\beta}^j \end{array} \right. \quad (15)$$

- (2) The number of divided regions of the target color image is less than the number of regions in the original color image.

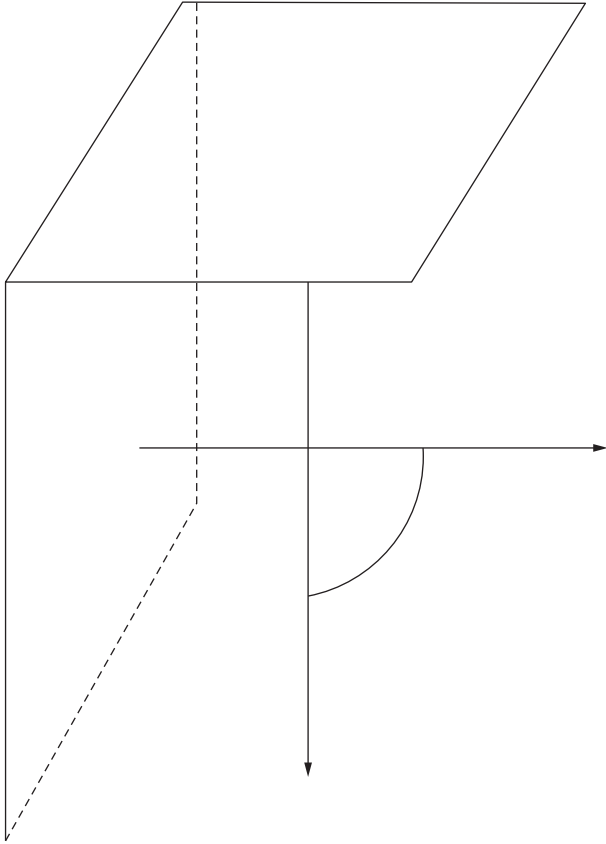


FIGURE 5: The concept of edge compatibility.

In order to prevent the problem of mismatching, effective adjustments need to be made for some mismatched areas.

The analysis of the overlap rate of the regional boundary is realized in the specific HSV color space in this study. The impact of sparseness is analyzed through the specific adjacent regions. The specific calculation can be obtained by the following formula:

$$H'_z = H_z + \sum \gamma_i (\mu_H^i - \mu_H^i). \quad (16)$$

If the  $j$ th area is adjacent to the  $i$ th area, the boundary overlap ratio of the  $j$ th area with respect to the  $i$ th area can be calculated by the following formula:

$$\gamma_{ij} = \frac{l_{ij}}{\sum_{n \in \psi} l_{in}}. \quad (17)$$

Among them,  $l_{ij}$  represents the length of the overlap boundary between the  $i$ th area and the  $j$ th area.

When the number of unmatched regions is large or the area of these regions is small, the color harmony in Section 4 of this study can be used to adjust the color of these regions. The details are shown in Figure 6.

**4.5. Optimization of Color Transfer Results Based on Color Harmony.** According to the color harmony theory, when the tones in the image are in the corresponding area of the

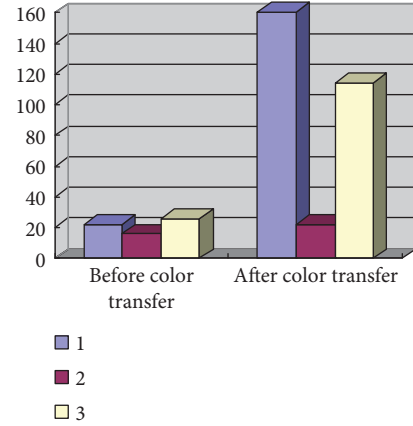


FIGURE 6: The mean value of tones and border overlap ratio in adjacent regions.

template, the color of the entire image gives people a more harmonious feeling [16–18]. On the basis of the existing research, the rotation angle of the suitable template and the color transfer without changing the color of the image can be realized. The specific steps mainly include

Step 1: first, the corresponding image needs to be converted into the color space of HSV, and the corresponding image is extracted for color circle diagram. The specific calculation is shown in the following formula:

$$F(X, (m, \tau)) = \sum_{p \in X} \|H(p) - E_{T_m(\tau)}(p)\| \cdot S(p). \quad (18)$$

Step 2: on the basis of step 1, the appropriate rotation angle of each template is analyzed and calculated. By selecting the discordant sparse template as the target template, the best rotation angle is determined to rotate the color harmony template.

Step 3: in order to effectively improve the harmony of the image, the color and the tone outside the harmony template can be effectively transferred and calculated through the tonal value. Specifically, it can be calculated by the following formula:

$$H'(p) = C(p) + \frac{w}{2} (1 - G_\sigma \|H(p) - C(p)\|). \quad (19)$$

It can be seen from the specific image tone results that the overall color change of the image is not obvious, but it can be seen from the details that the corresponding details have been partially adjusted to make the changes in this area more harmonious and enhance the harmony of the color transfer results [19, 20].

## 5. Experiment and Result Analysis

**5.1. Comparative Experiment of Each Step of the Algorithm in This Paper.** In terms of region matching, a specific color transfer result image can be obtained according to the specific matching result [17, 21, 22]. It can be seen from the

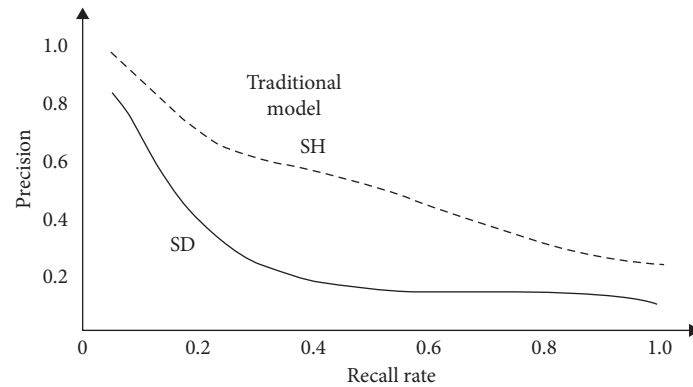


FIGURE 7: Traditional model curve.

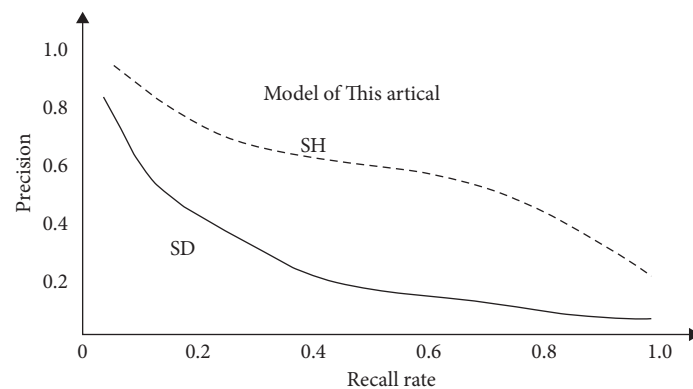


FIGURE 8: Precision-recall curve of the retrieval model in this study.

results that the matching algorithm can be used to obtain a simpler sensory experience compared to the regional results corresponding to the unadjusted initial matching. From the color transfer results, the topological information area matching model can significantly improve the overall color transfer effect of the image, ensuring that the color composition of the transferred image is closer to the specific target color graphics and makes people feel comfortable and harmonious.

**5.2. Comparison with Experimental Results of Other Algorithms.** In order to verify the efficiency of the algorithm, the corresponding curves for algorithm comparison is constructed by trial in this study while the topological relationship of the surfaces is considered to ensure that there are more surfaces constituting the model and to achieve effective interior design color transfer, as shown in Figures 7 and 8. From the comparison result, the topological information area matching model in this study is effective and can support CAD interior design color transfer simulation.

**5.3. Master the Design and Operation Skills.** For the two designers, on the one hand, they need to master the CAD drawing skills, that is, the computer is used to select a fixed target to expand and contract the screen as needed. For the result of the mouse, the window operation can be realized by dragging the layer. In the specific operation practice, you can

effectively frame selection through the regular image. On the other hand, the designer needs to delete and cancel software effectively [23, 24]. If it is in the execution state during the drawing operation, the operation target can be determined.

**5.4. Flexible Use of Design Templates.** At the same time, designers need to fully understand the business requirements, especially the business operation rules of interior design, and carry out the drawing frame design, the clear title, and the selection of the line type by following the corresponding standard design, in order to obtain flexible and available template, and finally clarify the auxiliary function. In the specific toolbar, the sketch design of the menu options can be realized, and the specific designers can capture the options to realize the specific environment design in order to realize the specific operation analysis.

**5.5. Unified Design Standards.** Although during the interior design process, specific CAD technology has obvious advantages over manual drawing; there is still a problem of inconsistent standards for different needs [25]. Therefore, cross-regional cooperation is relatively difficult; especially in specific drawing process, there is difficulty in unifying the labeling method and data connection. Therefore, emphasize shall be laid to the CAD coordination of interior design, to improve the drawing efficiency, and to achieve the effective unification of the standards.

**5.6. Highlight Integrated Design Advantage.** In the specific process of using CAD software, the goal of high integration cannot be achieved. The software design is used for horizontally integrated analysis. Different users can effectively perform the same task for analysis and realize the effective sharing and unified access of ports and realize the collaborative integrated analysis, while ensuring the communication and transmission of information and data and improving the quality of software design.

## 6. Conclusions

With the continuous development of social economy, interior design has received more and more attention as an important decoration link; especially when different styles appear, interior design pays more attention to color matching. In view of these shortcomings and limitations, a topological information area matching model analysis. Different is introduced in this study, which is different from the traditional global algorithm and local segmentation algorithm. The relationship between image regions is clarified, and the importance of color transfer is controlled through analyzing the business logic of interior design. Effective color transfer is performed according to specific needs, to realize regional color adjustment, achieve the effectiveness and completeness of color transfer, implement specific result impact analysis according to specific color methods, and improve transfer simulation and analysis of color. The simulation experiment results show that the topological information area matching model color is effective, can ensure the true color of the image color, and support the CAD interior design color transfer simulation.

## Data Availability

The labeled dataset used to support the findings of this study are available from the corresponding author upon request.

## Conflicts of Interest

The author declares no conflicts of interest.

## Acknowledgments

This study was sponsored by Yancheng Polytechnic College.

## References

- [1] M. Lee and Q. Fang, Y. Cho, J. Ryu, L. Liu, and D. S. Kim, Support-free hollowing for 3D printing via voronoi diagram of ellipses,” *Computer-Aided Design*, vol. 101, no. 3, pp. 23–36, 2017.
- [2] C. Bolchini, L. Cassano, P. Garza, E. Quintarelli, and F. Salice, “An expert CAD flow for incremental functional diagnosis of complex electronic boards,” *IEEE Transactions on Computer-Aided Design of Integrated Circuits and Systems*, vol. 34, no. 5, pp. 835–848, 2015.
- [3] S Wang, S Ki, and K Lee, “Configuration design sensitivity analysis for dynamic systems using CAD-based velocity field,” *AIAA Journal*, vol. 40, no. 6, pp. 1241–1244, 2015.
- [4] C. H. Eng, T. W. H. Backman, C. B Bailey, and C. Magnan, H. G. Martin, L. Katz, P. Baldi, and J. D. Keasling, ClusterCAD: a computational platform for type I modular polypeptide synthase design[J],” *Nucleic Acids Research*, vol. 2, no. 1, pp. 509–518, 2018.
- [5] B. C. Kim, Y. Jeon, S. Park, H. Tejjgeler, D. Leal, and D. Mun, “Toward standardized exchange of plant 3D CAD models using ISO 15926,” *Computer-Aided Design*, vol. 83, no. 1, pp. 80–95, 2017.
- [6] M. A. Zboinska, “Hybrid CAD/E platform supporting exploratory architectural design,” *Computer-Aided Design*, vol. 59, no. 3, pp. 64–84, 2015.
- [7] G. Sombrio, C. A. D. Pomar, L. S. de Oliveira, A. L. M. Freitas, F. L. Souza, and J. A. Souza, “Novel design of photocatalyst coaxial ferromagnetic core and semiconducting shell microwire architecture,” *Journal of Catalysis*, vol. 370, no. 3, pp. 61–69, 2019.
- [8] S. Kwon, B. C. Kim, D. Mun, and S. Han, “Simplification of feature-based 3D CAD assembly data of ship and offshore equipment using quantitative evaluation metrics,” *Computer-Aided Design*, vol. 59, no. 3, pp. 140–154, 2015.
- [9] S. Ghadai, A. Balu, S. Sarkar, and A. Krishnamurthy, “Learning localized features in 3D CAD models for manufacturability analysis of drilled holes,” *Computer Aided Geometric Design*, vol. 62, no. 5, pp. 263–275, 2018.
- [10] C González-Lluch, P Company, M Contero, J. D. Camba, and R. Plumed, “A Survey on 3D CAD model quality assurance and testing tools,” *Computer-Aided Design*, vol. 4, no. 5, pp. 64–79, 2016.
- [11] A. J. Gougoutas, N. Bastidas, S. P. Bartlett, and O. Jackson, “The use of computer-aided design/manufacturing (CAD/CAM) technology to aid in the reconstruction of congenitally deficient pediatric mandibles: a case series - ScienceDirect,” *International Journal of Pediatric Otorhinolaryngology*, vol. 79, no. 12, pp. 2332–2342, 2015.
- [12] L. D. Rasmussen, S. Winther, J. Westra et al., “Danish study of Non-Invasive testing in Coronary Artery Disease 2 (DANICAD 2): study design for a controlled study of diagnostic accuracy,” *American Heart Journal*, vol. 215, no. 3, pp. 114–128, 2019.
- [13] F. Y. Su, J. C. Tsai, D. Morton, and W. S. Lin, “Use of an open-source CAD software program and additive manufacturing technology to design and fabricate a definitive cast for retrofitting a crown to an existing removable partial denture,” *The Journal of prosthetic dentistry*, vol. 122, no. 4, pp. 351–354, 2019.
- [14] D. Kim, J. Park, and K. H. Ko, “Development of an AR based method for augmentation of 3D CAD data onto a real ship block image,” *Computer-Aided Design*, vol. 98, no. 5, pp. 1–11, 2018.
- [15] H. Y. Jeong, H. H. Lee, and Y. S. Choi, “Mechanical properties of hybrid computer-aided design/computer-aided manufacturing (CAD/CAM) materials after aging treatments,” *Ceramics International*, vol. 44, no. 3, pp. 272–288, 2018.
- [16] B. K. Ertürk, M. E. Çömlekoğlu, M. D. Çömlekoğlu, A. Aladağ, and M. A. Güngör, “A customized zirconia abutment design combined with a CAD/CAM laminate veneer: a clinical report,” *The International Journal of Periodontics & Restorative Dentistry*, vol. 35, no. 2, pp. 201–209, 2015.
- [17] Y. Yang, Z. Yang, J. Zhou, L. Chen, and J. Tan, “Effect of tooth preparation design on marginal adaptation of composite resin CAD-CAM onlays,” *The Journal of Prosthetic Dentistry*, vol. 124, no. 1, pp. 88–93, 2020.

- [18] W. Han, Y. Li, and Y. Zhang, "Design and fabrication of complete dentures using CAD/CAM technology," *Medicine*, vol. 96, no. 1, pp. 5435–5445, 2017.
- [19] W. S. Lin, B. T. Harris, K. Phasuk, D. R. Llop, and D. Morton, "Integrating a facial scan, virtual smile design, and 3D virtual patient for treatment with CAD-CAM ceramic veneers: a clinical report," *The Journal of Prosthetic Dentistry*, vol. 3, no. 4, pp. 1–9, 2018.
- [20] L. Sun, C. M. Tierney, C. G. Armstrong, and T. T. Robinson, "Decomposing complex thin-walled CAD models for hexahedral-dominant meshing," *Computer-Aided Design*, vol. 4, no. 3, pp. 118–131, 2017.
- [21] J. H. Lee, "Design concept for preventing aspiration or ingestion of CAD-CAM crowns: a dental technique," *The Journal of Prosthetic Dentistry*, vol. 123, no. 2, pp. 209–218, 2019.
- [22] None, "Design and fabrication of complete dentures using CAD/CAM technology," *Medicine*, vol. 96, no. 3, pp. 6030–6038, 2017.
- [23] A. Guy, H. Labelle, S. Barchi et al., "Braces designed using CAD/CAM combined or not with finite element modeling lead to effective treatment and quality of life after 2 Years: a randomized controlled trial," *Spine*, vol. 46, no. 3, pp. 109–118, 2021.
- [24] B. Patel, A. Patel, A. Patel, and H. Bhatt, "CoMFA, CoMSIA, molecular docking and MOLCAD studies of pyrimidinone derivatives to design novel and selective tankyrase inhibitors," *Journal of Molecular Structure*, vol. 1221, no. 3, pp. 128–137, 2020.
- [25] X. Zhu, Y. Ji, C. Zhu, P. Hu, and Z. D. Ma, "Isogeometric analysis for trimmed CAD surfaces using multi-sided toric surface patches," *Computer Aided Geometric Design*, vol. 79, no. 3, pp. 101–118, 2020.